A partial wave analysis of the centrally produced K^+K^- and $K^0\_sK^0\_s$ systems in pp interactions at 450 GeV/c and new information on the spin of the f_1 (1710)

D. Barberis, W. Beusch, F G. Binon, a M. Blick, F E. Close, K M. Danielsen, a V. Dolgopolov, S V. Donskov, B C. Earl, D. Evans, et al.

10 February 1999

A partial wave analysis of the centrally produced K^+K^- and $K^0_SK^0_S$ systems in pp interactions at 450 GeV/c and new information on the spin of the $f_J(1710)$

The WA102 Collaboration

D. Barberis[4], W. Beusch[4], F.G. Binon[6], A.M. Blick[5], F.E. Close[3,4], K.M. Danielsen[10], A.V. Dolgopolov[5], S.V. Donskov[5], B.C. Earl[3], D. Evans[3], B.R. French[4], T. Hino[11], S. Inaba[8], A.V. Inyakin[5], T. Ishida[8], A. Jacholkowski[4], T. Jacobsen[10], G.T Jones[3], G.V. Khaustov[5], T. Kinashi[12], J.B. Kinson[3], A. Kirk[3], W. Klempt[4], V. Kolosov[5], A.A. Kondashov[5], A.A. Lednev[5], V. Lenti[4], S. Maljukov[7], P. Martinengo[4], I. Minashvili[7], T. Nakagawa[11], K.L. Norman[3], J.P. Peigneux[1], S.A. Polovnikov[5], V.A. Polyakov[5], V. Romanovsky[7], H. Rotscheidt[4], V. Rumyantsev[7], N. Russakovich[7], V.D. Samoylenko[5], A. Semenov[7], M. Sené[4], R. Sené[4], P.M. Shagin[5], H. Shimizu[12], A.V. Singovsky[1,5], A. Sobol[5], A. Solovjev[7], M. Stassinaki[2], J.P. Stroot[6], V.P. Sugonyaev[5], K. Takamatsu[9], G. Tchlatchidze[7], T. Tsuru[8], M. Venables[3], O. Villalobos Baillie[3], M.F. Votruba[3], Y. Yasu[8].

Abstract

A partial wave analysis of the centrally produced K^+K^- and $K^0_SK^0_S$ channels has been performed in pp collisions using an incident beam momentum of 450 GeV/c. An unambiguous physical solution has been found in each channel. The striking feature is the observation of peaks in the S-wave corresponding to the $f_0(1500)$ and $f_J(1710)$ with J = 0. The D-wave shows evidence for the $f_2(1270)/a_2(1320)$, the $f'_2(1525)$ and the $f_2(2150)$ but there is no evidence for a statistically significant contribution in the D-wave in the 1.7 GeV mass region.

Submitted to Physics Letters

1 LAPP-IN2P3, Annecy, France.
2 Athens University, Physics Department, Athens, Greece.
3 School of Physics and Astronomy, University of Birmingham, Birmingham, U.K.
4 CERN - European Organization for Nuclear Research, Geneva, Switzerland.
5 IHEP, Protvino, Russia.
6 IISN, Belgium.
7 JINR, Dubna, Russia.

[8] High Energy Accelerator Research Organization (KEK), Tsukuba, Ibaraki 305, Japan.
[9] Faculty of Engineering, Miyazaki University, Miyazaki, Japan.
[10] Oslo University, Oslo, Norway.
[11] Faculty of Science, Tohoku University, Aoba-ku, Sendai 980, Japan.
[12] Faculty of Science, Yamagata University, Yamagata 990, Japan.

One of the fundamental predictions of QCD is the existence of glueballs. Current theoretical predictions based on lattice gauge calculations indicate that the lowest lying scalar glueball should be in the mass range 1500-1700 MeV [1]. The $f_0(1500)$ and the $f_J(1710)$ display clear glueball characteristics in that they are both produced in glue-rich production mechanisms and are either not seen, or are heavily suppressed in normal hadronic interactions. In addition, the $f_J(1710)$ is observed to decay dominantly to $K\overline{K}$ and yet it is not produced in K^-p interactions [2]. However, the spin of the $f_J(1710)$ is still uncertain with J = 0 or 2 being possible.

In 1987 the MARK III collaboration published the results of a spin analysis of the $f_J(1710)$ observed in radiative J/ψ decays [3]. The analysis assumed that the $f_J(1710)$ region was pure spin zero or pure spin two and ignored interference effects. The results from the spin analysis showed that spin two was preferred over spin zero.

In 1989 the WA76 collaboration published results from the analysis of the centrally produced $K\overline{K}$ system [4]. In an attempt to assess the spin of the $f_J(1710)$ the angular distributions in the 1.5 and 1.7 GeV mass regions were studied. The angular distributions in the two mass regions were found to be similar, and since it was assumed that the signal at 1.5 GeV was due to the $f_2'(1525)$, it was concluded that the signal at 1.7 GeV was also spin two. From these two observations the $f_J(1710)$ was allocated spin two.

A more sophisticated analysis of the Mark III data [5] including both spin zero and two amplitudes and the possibility of interference between them showed that the 1.7 GeV mass region was dominated by spin zero. However, these analyses have only ever been published in conference proceedings and have never been followed up with publications in refereed journals.

More recently, the E690 experiment at Fermilab has published the results of a partial wave analysis of the centrally produced $K_S^0K_S^0$ system [6]. The mass spectrum looks very similar to that of the WA76 experiment; however, the peak at 1.5 GeV is found to have spin zero and not spin two as had been assumed in the WA76 analysis. Unfortunately, above 1.58 GeV, due to an ambiguity in the solutions, a unique determination of the spin of the $f_J(1710)$ could not be made by E690.

It is essential to know the spin of the $f_J(1710)$ because measurements of its production rate in J/ψ decays indicates that if it has spin two then it would be consistent with being a normal $q\overline{q}$ meson whereas if it has spin zero it would be consistent with having a significant glueball component [7].

This paper presents a study of the K^+K^- and $K_S^0K_S^0$ final states formed in the reaction

$$pp \rightarrow p_f(K\overline{K})p_s \tag{1}$$

at 450 GeV/c. The subscripts f and s indicate the fastest and slowest particles in the laboratory respectively. The WA102 experiment has been performed using the CERN Omega Spectrometer, the layout of which is described in ref. [8].

The reaction

$$pp \rightarrow p_f(K^+K^-)p_s \tag{2}$$

has been isolated from the sample of events having four outgoing charged tracks, by first imposing the following cuts on the components of the missing momentum: |missing P_x| < 14.0

GeV/c, |missing P_y| < 0.16 GeV/c and |missing P_z| < 0.08 GeV/c, where the x axis is along the beam direction. A correlation between pulse-height and momentum obtained from a system of scintillation counters was used to ensure that the slow particle was a proton.

In order to select the K^+K^- system, information from the Čerenkov counter was used. One centrally produced charged particle was required to be identified as an ambiguous K/p by the Čerenkov counter and the other particle was required to be consistent with being a kaon. The largest contamination to the real K^+K^- final state comes from the reaction $pp \to \Delta_f^{++} p_s \pi^-$ where the high momentum π^+ from the decay of the Δ^{++} is misidentified as a K by the Čerenkov system. In order to reject this contamination the positive particle was assigned the π mass and the $\Delta^{++}(1232)$ signal has been removed by requiring $M(p_f\pi^+) > 1.5$ GeV.

The method of Ehrlich et al. [9], has been used to compute the mass squared of the two centrally produced particles assuming them to have equal mass. The resulting distribution is shown in fig. 1a) where peaks can be seen at the π, K and p masses squared. A cut on the Ehrlich mass squared of $0.14 \leq M_X^2 \leq 0.55\ GeV^2$ has been used to select a sample of 30 868 K^+K^- events.

The peak at the π mass squared results from πs being misidentified as Ks by an inefficiency of the Čerenkov counter. To determine the contamination from these $\pi^+\pi^-$ events inside the Ehrlich mass cut, real $\pi^+\pi^-$ events have been passed through a simulation of the apparatus in which the efficiency of the Čerenkov counter (94 ± 1 %) has been taken into account. The resulting distribution is shown as the shaded histogram in fig. 1a). The amount of contamination is small and the effect this contamination has on the angular distribution has been found to be negligible [10].

The centrally produced K^+K^- effective mass distribution is shown in fig. 1b). The main features of the spectrum are evidence for a sharp threshold enhancement and peaks in the 1.5 and 1.7 GeV regions.

A Partial Wave Analysis (PWA) of the centrally produced K^+K^- system has been performed assuming the K^+K^- system is produced by the collision of two particles (referred to as exchanged particles) emitted by the scattered protons. The z axis is defined by the momentum vector of the exchanged particle with the greatest four-momentum transferred in the K^+K^- centre of mass. The y axis is defined by the cross product of the two exchanged particles in the pp centre of mass. The two variables needed to specify the decay process were taken as the polar and azimuthal angles (θ, ϕ) of the K^- in the K^+K^- centre of mass relative to the coordinate system described above.

The acceptance corrected moments, defined by

$$I(\Omega) = \sum_L t_{L0} Y_L^0(\Omega) + 2 \sum_{L,M>0} t_{LM} Re\{Y_L^M(\Omega)\} \tag{3}$$

have been rescaled to the total number of observed events and are shown in fig. 2. As can be seen the moments with $M > 2$ and $L > 4$ are small (i.e. t_{43}, t_{44}, t_{50} and t_{60}) and hence only S, P, and D waves with $m \leq 1$ have been included in the PWA. The t_{00} moment represents the total acceptance corrected mass spectrum. As can be seen, by comparing this spectrum with the raw mass spectrum shown in fig. 1b), the effect of the acceptance is to increase the

proportion of events with masses less than 1.3 GeV. This is mainly due to the effects of the momentum threshold of the Čerenkov counter.

The amplitudes used for the PWA are defined in the reflectivity basis [11]. In this basis the angular distribution is given by a sum of two non-interfering terms corresponding to negative and positive values of reflectivity. The waves used were of the form J^{ε}_{m} with J = S, P and D, $m = 0, 1$ and reflectivity $\varepsilon = \pm 1$. The expressions relating the moments (t_{LM}) and the waves (J^{ε}_{m}) are given in table 1. Since the overall phase for each reflectivity is indeterminate, one wave in each reflectivity can be set to be real (S^{-}_{0} and P^{+}_{1} for example) and hence two phases can be set to zero ($\phi_{S^{-}_{0}}$ and $\phi_{P^{+}_{1}}$ have been chosen). This results in 12 parameters to be determined from the fit to the angular distributions.

The PWA has been performed independently in 40 MeV intervals of the $K^{+}K^{-}$ mass spectrum. In each mass bin an event-by-event maximum likelihood method has been used. The function

$$F = -\sum_{i=1}^{N} ln\{I(\Omega)\} + \sum_{L,M} t_{LM}\epsilon_{LM} \tag{4}$$

has been minimised, where N is the number of events in a given mass bin, ϵ_{LM} are the efficiency corrections calculated in the centre of the bin and t_{LM} are the moments of the angular distribution. The moments calculated from the partial amplitudes are shown superimposed on the experimental moments in fig 2. As can be seen the results of the fit reproduce well the experimental moments.

The equations that express the moments via the partial wave amplitudes form a non-linear system that leads to inherent ambiguities. For a system with S, P and D waves there are eight solutions for each mass bin. In each mass bin one of these solutions is found from the fit to the experimental angular distributions; the other seven can then be calculated by the method described in ref. [11]. In order to link the solutions in adjacent mass bins, the real and imaginary parts of the Barrelet function roots are required to be step-wise continuous and have finite derivatives as a function of mass [12]. By definition all the solutions give identical moments and identical values of the likelihood. The only way to differentiate between the solutions, if different, is to apply some external physical test, such as requiring that at threshold the S-wave is the dominant wave.

The four complex roots, Z_i, after the linking procedure are shown in fig. 1c) and d). As can be seen the imaginary parts give little help in the linking procedure. However, the real parts are well separated in most places and hence it is possible to identify unambiguously all the PWA solutions in the whole mass range. In the 1.8 GeV mass region two roots do become close together, but if these two roots are swapped it results in events from the S-wave being transferred almost entirely into the P-wave and produces mass spectra that look unphysical. In addition, the zeros do not cross the real axis and hence there is no problem with bifurcation of the solutions. Near threshold the P-wave is the dominant contribution for five out of eight solutions, another is dominated by D-wave and another has the same amount of S-wave and P-wave. These seven solutions [10] have been ruled out because the $K^{+}K^{-}$ cross section near threshold has been assumed to be dominated by S-wave. The remaining solution is shown in fig. 3.

The S-wave shows a threshold enhancement; the peaks at 1.5 GeV and 1.7 GeV are inter-

preted as being due to the $f_0(1500)$ and $f_J(1710)$ with J = 0. The D-wave shows peaks in the 1.3 and 1.5 GeV regions, presumably due to the $f_2(1270)/a_2(1320)$ and $f_2'(1525)$ and a wide structure above 2 GeV. There is no evidence for any significant structure in the D-wave in the region of the $f_J(1710)$. In addition, there are no statistically significant structures in any of the other waves.

Extensive Monte Carlo simulations have been performed to check the validity of this result. They show that the feed through from the S-wave to the D-wave is approximately 5 % from threshold to 1.3 GeV decreasing to less than 1 % for masses greater than 1.5 GeV. The feed through from D-wave to S-wave is found to be negligible over the entire mass range and hence gives confidence in the above observation that the $f_J(1710)$ has J = 0.

A fit has been performed to the S_0^- wave using three interfering Breit-Wigners to describe the $f_0(980)$, $f_0(1500)$ and $f_J(1710)$ and a background of the form $a(m-m_{th})^b exp(-cm-dm^2)$, where m is the K^+K^- mass, m_{th} is the K^+K^- threshold mass and a, b, c, d are fit parameters. The Breit-Wigners have been convoluted with a Gaussian to account for the experimental mass resolution (σ = 6 MeV at threshold rising to 19 MeV at 2 GeV). The resulting fit is shown in fig. 4a) and gives

$f_0(980)$	M	=	985	±	10	MeV,	Γ	=	65 ± 20	MeV
$f_0(1500)$	M	=	1497	±	10	MeV,	Γ	=	104 ± 25	MeV
$f_0(1710)$	M	=	1730	±	15	MeV,	Γ	=	100 ± 25	MeV

parameters which are consistent with the PDG [13] values for these resonances.

A fit has been performed to the D_0^- wave above 1.2 GeV using three incoherent relativistic spin 2 Breit-Wigners to describe the $f_2(1270)/a_2(1320)$, $f_2'(1525)$ and the peak at 2.2 GeV a background of the form $a(m-m_{th})^b exp(-cm-dm^2)$, where m is the K^+K^- mass, m_{th} is the K^+K^- threshold mass and a, b, c, d are fit parameters. The resulting fit is shown in fig. 4b) and gives

$f_2(1270)/a_2(1320)$	M	=	1305	±	20	MeV,	Γ	=	132 ± 25	MeV
$f_2'(1525)$	M	=	1515	±	15	MeV,	Γ	=	70 ± 25	MeV
$f_2(2150)$	M	=	2130	±	35	MeV,	Γ	=	270 ± 50	MeV.

The parameters for the peak at 1.3 GeV fall between the PDG [13] values for the $f_2(1270)$ and $a_2(1320)$. The values for the $f_2'(1525)$ are compatible with the PDG values and those for the structure at 2.15 GeV are compatible with both the $f_2(2150)$ and with the parameters for the structure seen in radiative J/ψ decays to the same channel [14].

A study has also been made of the centrally produced $K_S^0K_S^0$ channel. This channel has lower statistics than the K^+K^- channel but has the advantage that only even spins can contribute, which also means that there are only two ambiguous solutions to the PWA. The reaction

$$pp \to p_f(K_S^0K_S^0)p_s \tag{5}$$

has been isolated from the sample of events having two outgoing charged tracks plus two V^0s, by first imposing the following cuts on the components of the missing momentum: |missing P_x| < 20.0 GeV/c, |missing P_y| < 0.16 GeV/c and |missing P_z| < 0.12 GeV/c.

The quantity Δ, defined as $\Delta = MM^2(p_f p_s) - M^2(K^0_S K^0_S)$, where $MM^2(p_f p_s)$ is the missing mass squared of the two outgoing protons, was then calculated for each event and a cut of $|\Delta| \leq 3.0$ (GeV)^2 was used to select the $K^0_S K^0_S$ channel. Requiring one V^0 to be compatible with being a K^0_S ($0.475 < M(\pi^+\pi^-) < 0.520$ GeV) the effective mass of the other V^0 is shown in fig 5a) where a clear K^0_S signal can be seen over little background. The resulting $K^0_S K^0_S$ effective mass spectrum is shown in fig. 5b) and consists of 2712 events.

A Partial Wave Analysis (PWA) of the centrally produced $K^0_S K^0_S$ system has then been performed assuming the same analysis frame as for the K^+K^- system. Since only even spins can contribute only S and D waves with $m \leq 1$ have been included in the PWA. The expressions relating the moments and the waves are given in table 2. The PWA has been performed independently in 80 MeV intervals of the $K^0_S K^0_S$ mass spectrum.

The two complex roots, Z_i, after the linking procedure, are shown in fig. 5c) and d). As in the case of the K^+K^- channel the real parts are well separated and hence it is possible to identify unambiguously the two PWA solutions in the whole mass range. In addition, the zeros do not cross the real axis and hence there is no problem with bifurcation of the solutions. For one solution the mass spectrum is evenly distributed through the three D-waves and the S-wave is small everywhere, this solution has been ruled out. The remaining solution is shown in fig. 5e)-h). As in the case of the K^+K^- final state, it can be seen that the S-wave shows a threshold enhancement; the peaks at 1.5 GeV and 1.7 GeV are interpreted as being due to the $f_0(1500)$ and $f_J(1710)$ with J = 0. Superimposed on the S-wave is the result of a fit using the parametrisation used to fit the K^+K^- S-wave. As can be seen this parametrisation describes the $K^0_S K^0_S$ S-wave.

In conclusion, a partial wave analysis of the centrally produced K^+K^- and $K^0_S K^0_S$ systems has been performed. An unambiguous physical solution has been found in each channel. The striking feature is the observation of peaks in the S-wave corresponding to the $f_0(1500)$ and $f_J(1710)$ with J = 0. The D-wave shows evidence for the $f_2(1270)/a_2(1320)$, the $f'_2(1525)$ and the $f_2(2150)$ but there is no evidence for a statistically significant contribution in the D-wave in the 1.7 GeV mass region.

Acknowledgements

This work is supported, in part, by grants from the British Particle Physics and Astronomy Research Council, the British Royal Society, the Ministry of Education, Science, Sports and Culture of Japan (grants no. 04044159 and 07044098), the Programme International de Co-operation Scientifique (grant no. 576) and the Russian Foundation for Basic Research (grants 96-15-96633 and 98-02-22032).

References

[1] G. Bali *et al.,* Phys. Lett. **B309** (1993) 378;

D. Weingarten, hep-lat/9608070;

J. Sexton *et al.,* Phys. Rev. Lett. **75** (1995) 4563;

F.E. Close and M.J. Teper, "On the lightest Scalar Glueball" Rutherford Appleton Laboratory report no. RAL-96-040; Oxford University report no. OUTP-96-35P

[2] Ph. Gavillet *et al.,* Zeit. Phys. **C16** (1982) 119;
D. Aston *et al.,* Nucl. Phys. **B301** (1988) 525.

[3] R.M. Baltrusaitis *et al.,* Phys. Rev. **D35** (1987) 2077.

[4] T.A. Armstrong *et al.,* Phys. Lett. **B227** (1989) 186.

[5] L.P. Chen *et al.,* Nucl. Phys. Proc. Suppl. **B21** (1991) 80;
L.P. Chen *et al.,* Proceedings of Hadron 91, Maryland, USA (1991) 26.;
W. Dunwoodie, Proceedings of Hadron 97, AIP Conf. Series 432 (1997) 753.

[6] M.A. Reyes *et al.,* Phys. Rev. Lett. **81** (1998) 4079.

[7] F.E. Close, G.R. Farrar and Z. Li, Phys. Rev. **D55** (1997) 5749.

[8] D. Barberis *et al.,* Phys. Lett. **B397** (1997) 339.

[9] R. Ehrlich *et al.,* Phys. Rev. Lett. **20** (1968) 686.

[10] B.C. Earl, Thesis, University of Birmingham, U.K. 1999.

[11] S.U. Chung, Phys. Rev. **D56** (1997) 7299.

[12] D. Alde *et al.,*, Europ. Phys. Journal. **A3** (1998) 361.

[13] Particle Data Group, European Physical Journal **C3** (1998) 1.

[14] R.M. Baltrusaitis *et al.,* Phys. Rev. Lett. **56** (1986) 107;
J.E. Augustin *et al.,* Phys. Rev. Lett. **60** (1988) 2238;
L. Kopke and N.Wermes, Phys. Rep. **174** (1989) 67.

Table 1: The moments of the angular distribution expressed in terms of the partial waves for the K^+K^- system.

$$
\begin{aligned}
\sqrt{4\pi}t_{00} &= |S_0^-|^2 + |P_0^-|^2 + |P_1^-|^2 + |P_1^+|^2 + |D_0^-|^2 + |D_1^-|^2 + |D_1^+|^2 \\
\sqrt{4\pi}t_{10} &= 2|S_0^-||P_0^-|cos(\phi_{S_0^-} - \phi_{P_0^-}) + \tfrac{4}{\sqrt{5}}|P_0^-||D_0^-|cos(\phi_{P_0^-} - \phi_{D_0^-}) \\
&\quad + \tfrac{2\sqrt{3}}{\sqrt{5}}\{|P_1^-||D_1^-|cos(\phi_{P_1^-} - \phi_{D_1^-}) + |P_1^+||D_1^+|cos(\phi_{P_1^+} - \phi_{D_1^+})\} \\
\sqrt{4\pi}t_{11} &= \sqrt{2}|S_0^-||P_1^-|cos(\phi_{S_0^-} - \phi_{P_1^-}) - \tfrac{\sqrt{2}}{\sqrt{5}}|P_1^-||D_0^-|cos(\phi_{P_1^-} - \phi_{D_0^-}) \\
&\quad + \tfrac{\sqrt{6}}{\sqrt{5}}|P_0^-||D_1^-|cos(\phi_{P_0^-} - \phi_{D_1^-}) \\
\sqrt{4\pi}t_{20} &= \tfrac{2}{\sqrt{5}}|P_0^-|^2 - \tfrac{1}{\sqrt{5}}(|P_1^-|^2 + |P_1^+|^2) + \tfrac{\sqrt{5}}{7}(2|D_0^-|^2 + |D_1^-|^2 + |D_1^+|^2) \\
&\quad + 2|S_0^-||D_0^-|cos(\phi_{S_0^-} - \phi_{D_0^-}) \\
\sqrt{4\pi}t_{21} &= \tfrac{\sqrt{6}}{\sqrt{5}}|P_1^-||P_0^-|cos(\phi_{P_1^-} - \phi_{P_0^-}) + \tfrac{\sqrt{10}}{7}|D_1^-||D_0^-|cos(\phi_{D_1^-} - \phi_{D_0^-}) \\
&\quad + \sqrt{2}|S_0^-||D_1^-|cos(\phi_{S_0^-} - \phi_{D_1^-}) \\
\sqrt{4\pi}t_{22} &= \tfrac{\sqrt{3}}{\sqrt{10}}(|P_1^-|^2 - |P_1^+|^2) + \tfrac{\sqrt{15}}{7\sqrt{2}}(|D_1^-|^2 - |D_1^+|^2) \\
\sqrt{4\pi}t_{30} &= -\tfrac{6}{\sqrt{35}}\{|P_1^-||D_1^-|cos(\phi_{P_1^-} - \phi_{D_1^-}) + |P_1^+||D_1^+|cos(\phi_{P_1^+} - \phi_{D_1^+})\} \\
&\quad + \tfrac{6\sqrt{3}}{\sqrt{35}}|P_0^-||D_0^-|cos(\phi_{P_0^-} - \phi_{D_0^-}) \\
\sqrt{4\pi}t_{31} &= \tfrac{6}{\sqrt{35}}|P_1^-||D_0^-|cos(\phi_{P_1^-} - \phi_{D_0^-}) + \tfrac{4\sqrt{3}}{\sqrt{35}}|P_0^-|D_1^-|cos(\phi_{P_0^-} - \phi_{D_1^-}) \\
\sqrt{4\pi}t_{32} &= \tfrac{\sqrt{6}}{\sqrt{7}}\{|P_1^-||D_1^-|cos(\phi_{P_1^-} - \phi_{D_1^-}) - |P_1^+||D_1^+|cos(\phi_{P_1^+} - \phi_{D_1^+})\} \\
\sqrt{4\pi}t_{40} &= \tfrac{6}{7}|D_0^-|^2 - \tfrac{4}{7}(|D_1^-|^2 + |D_1^+|^2) \\
\sqrt{4\pi}t_{41} &= \tfrac{2\sqrt{15}}{7}|D_0^-||D_1^-|cos(\phi_{D_0^-} - \phi_{D_1^-}) \\
\sqrt{4\pi}t_{42} &= \tfrac{\sqrt{10}}{7}(|D_1^-|^2 - |D_1^+|^2)
\end{aligned}
$$

Table 2: The moments of the angular distribution expressed in terms of the partial waves for the $K_S^0 K_S^0$ system.

$$
\begin{aligned}
\sqrt{4\pi}t_{00} &= |S_0^-|^2 + |D_0^-|^2 + |D_1^-|^2 + |D_1^+|^2 \\
\sqrt{4\pi}t_{20} &= \tfrac{\sqrt{5}}{7}(2|D_0^-|^2 + |D_1^-|^2 + |D_1^+|^2) \\
&\quad +2|S_0^-||D_0^-|cos(\phi_{S_0^-} - \phi_{D_0^-}) \\
\sqrt{4\pi}t_{21} &= \tfrac{\sqrt{10}}{7}|D_1^-||D_0^-|cos(\phi_{D_1^-} - \phi_{D_0^-}) \\
&\quad +\sqrt{2}|S_0^-||D_1^-|cos(\phi_{S_0^-} - \phi_{D_1^-}) \\
\sqrt{4\pi}t_{22} &= \tfrac{\sqrt{15}}{7\sqrt{2}}(|D_1^-|^2 - |D_1^+|^2) \\
\sqrt{4\pi}t_{40} &= \tfrac{6}{7}|D_0^-|^2 - \tfrac{4}{7}(|D_1^-|^2 + |D_1^+|^2) \\
\sqrt{4\pi}t_{41} &= \tfrac{2\sqrt{15}}{7}|D_0^-||D_1^-|cos(\phi_{D_0^-} - \phi_{D_1^-}) \\
\sqrt{4\pi}t_{42} &= \tfrac{\sqrt{10}}{7}(|D_1^-|^2 - |D_1^+|^2)
\end{aligned}
$$

Figures

Figure 1: a) The Ehrlich mass squared distribution and b) the K^+K^- mass spectrum. The c) Real and d) Imaginary parts of the roots (see text) as a function of mass obtained from the PWA of the K^+K^- system.

Figure 2: The $\sqrt{4\pi}t_{LM}$ moments from the data. are the resulting moments calculated from the PWA of the K^+K^- final state.

Figure 3: The physical solution from the PWA of the K^+K^- final state.

Figure 4: The a) S_0^- and b) D_0^- waves with fits described in the text.

Figure 5: The $K_S^0K_S^0$ final state. a) the $M(\pi^+\pi^-)$ mass spectrum when the other V^0 is compatible with being a K_S^0. b) The $K_S^0K_S^0$ mass spectrum. The c) Real and d) Imaginary parts of the roots (see text) as a function of mass obtained from the PWA of the $K_S^0K_S^0$ system. e)-h) The physical solution from the PWA of the $K_S^0K_S^0$ system.

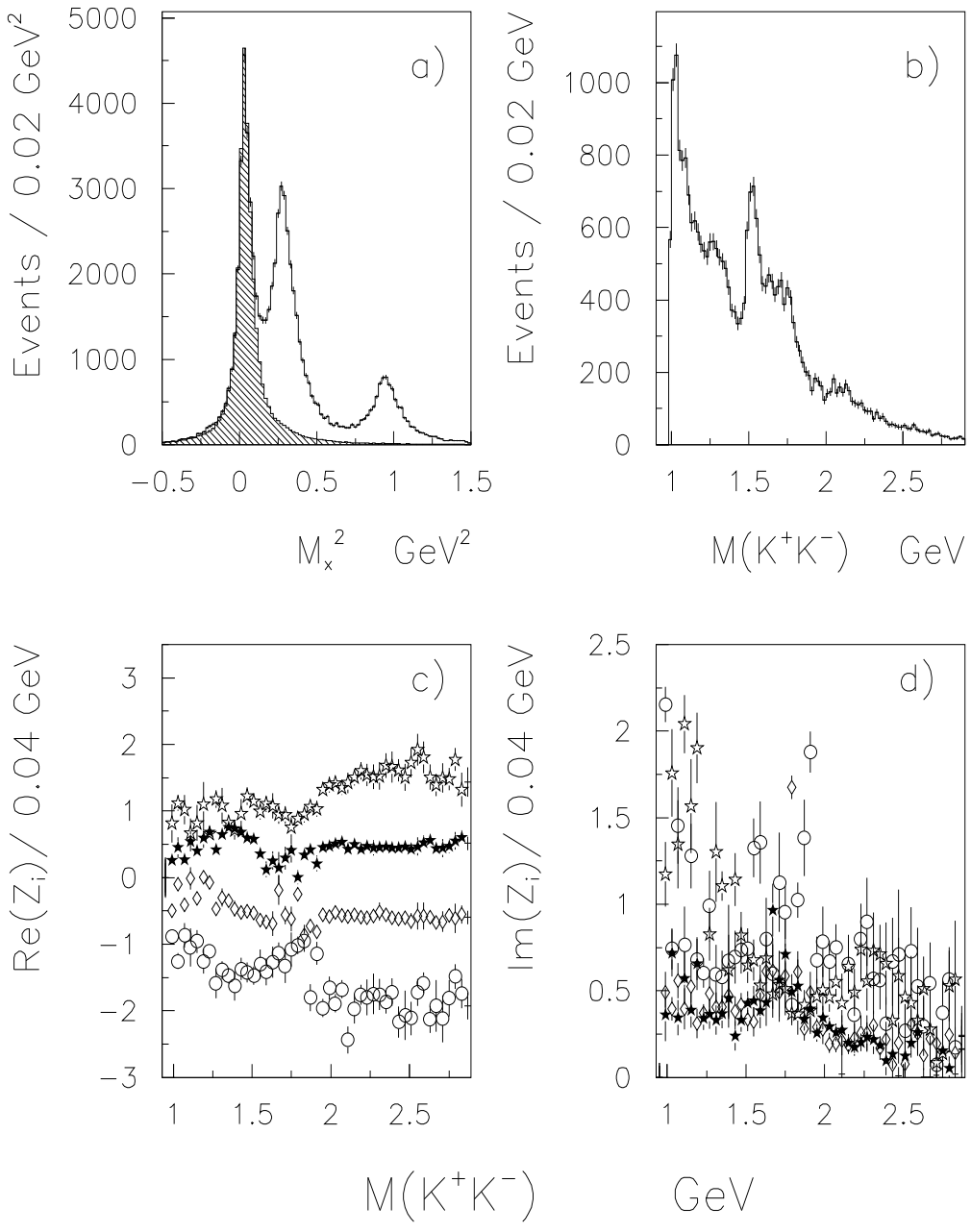
a)
b)
c)
d)
Events / 0.02 GeV²
Events / 0.02 GeV
Re(Z_i)/ 0.04 GeV
Im(Z_i)/ 0.04 GeV
M_x² GeV²
M(K⁺K⁻) GeV

Figure 1

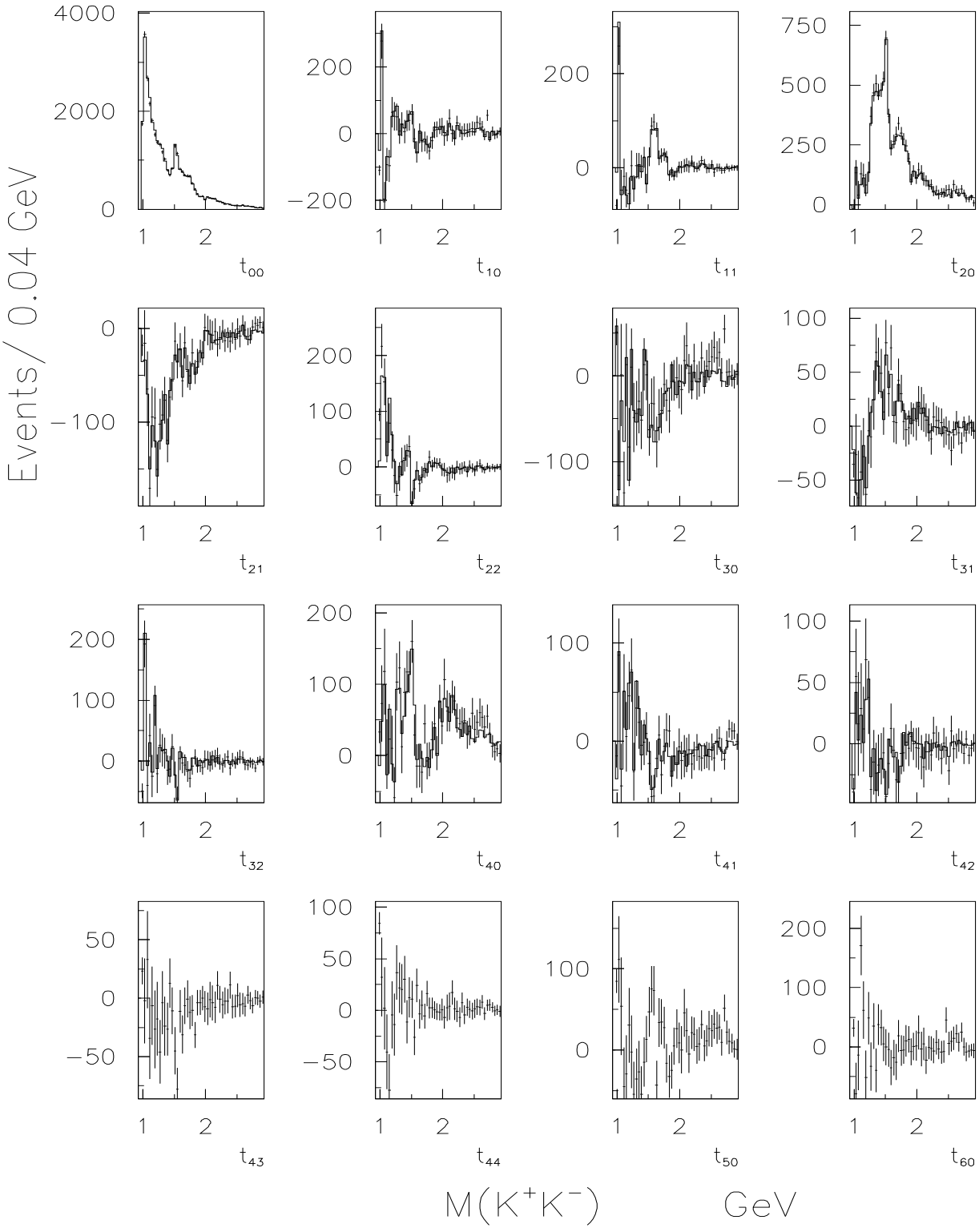
Events/ 0.04 GeV
M(K+K−) GeV
t00
t10
t11
t20
t21
t22
t30
t31
t32
t40
t41
t42
t43
t44
t50
t60

Figure 2

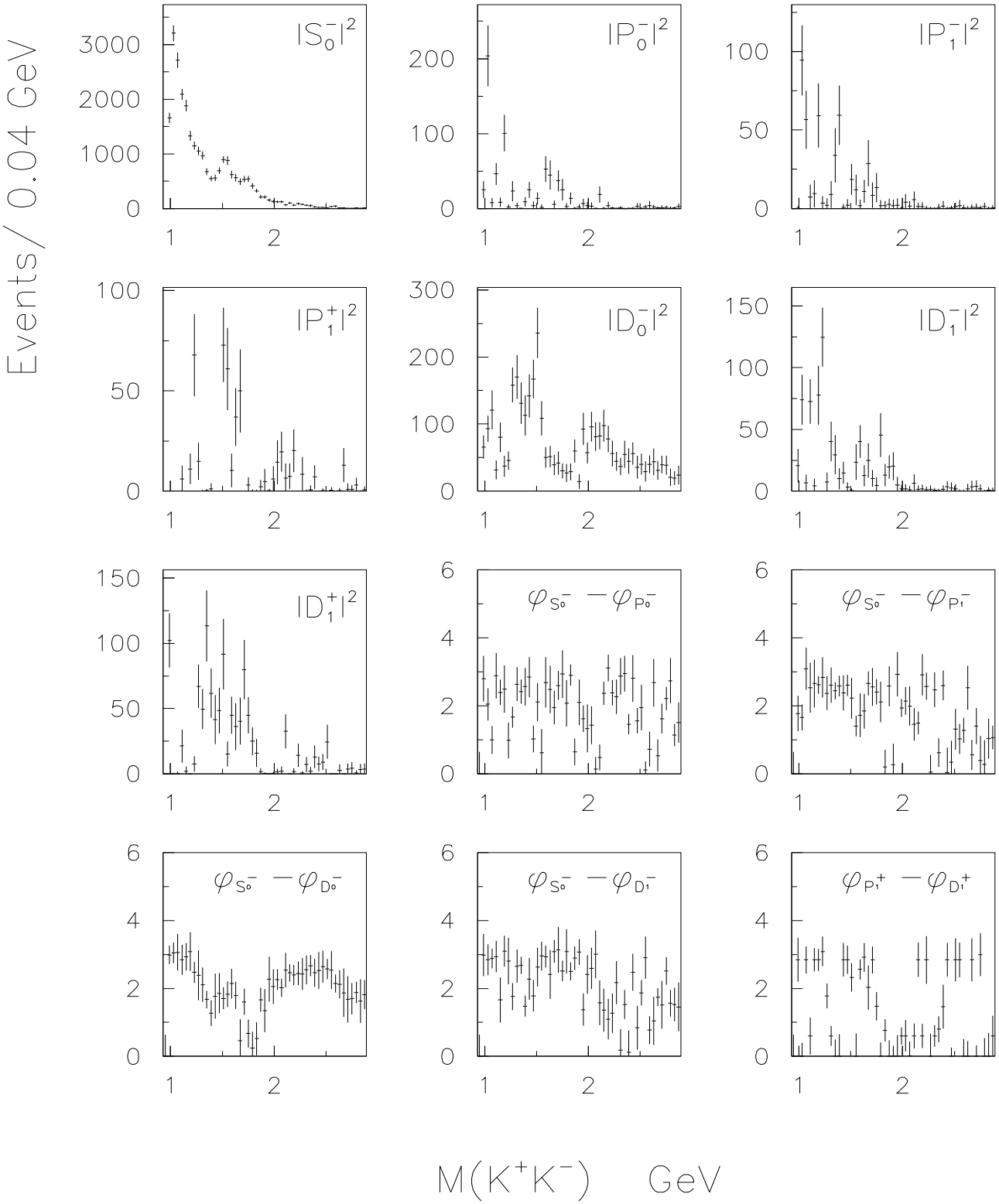
Events / 0.04 GeV
$|S_0^-|^2$
$|P_0^-|^2$
$|P_1^-|^2$
$|P_1^+|^2$
$|D_0^-|^2$
$|D_1^-|^2$
$|D_1^+|^2$
$\varphi_{S_0^-} - \varphi_{P_0^-}$
$\varphi_{S_0^-} - \varphi_{P_1^-}$
$\varphi_{S_0^-} - \varphi_{D_0^-}$
$\varphi_{S_0^-} - \varphi_{D_1^-}$
$\varphi_{P_1^+} - \varphi_{D_1^+}$
M(K⁺K⁻) GeV

Figure 3

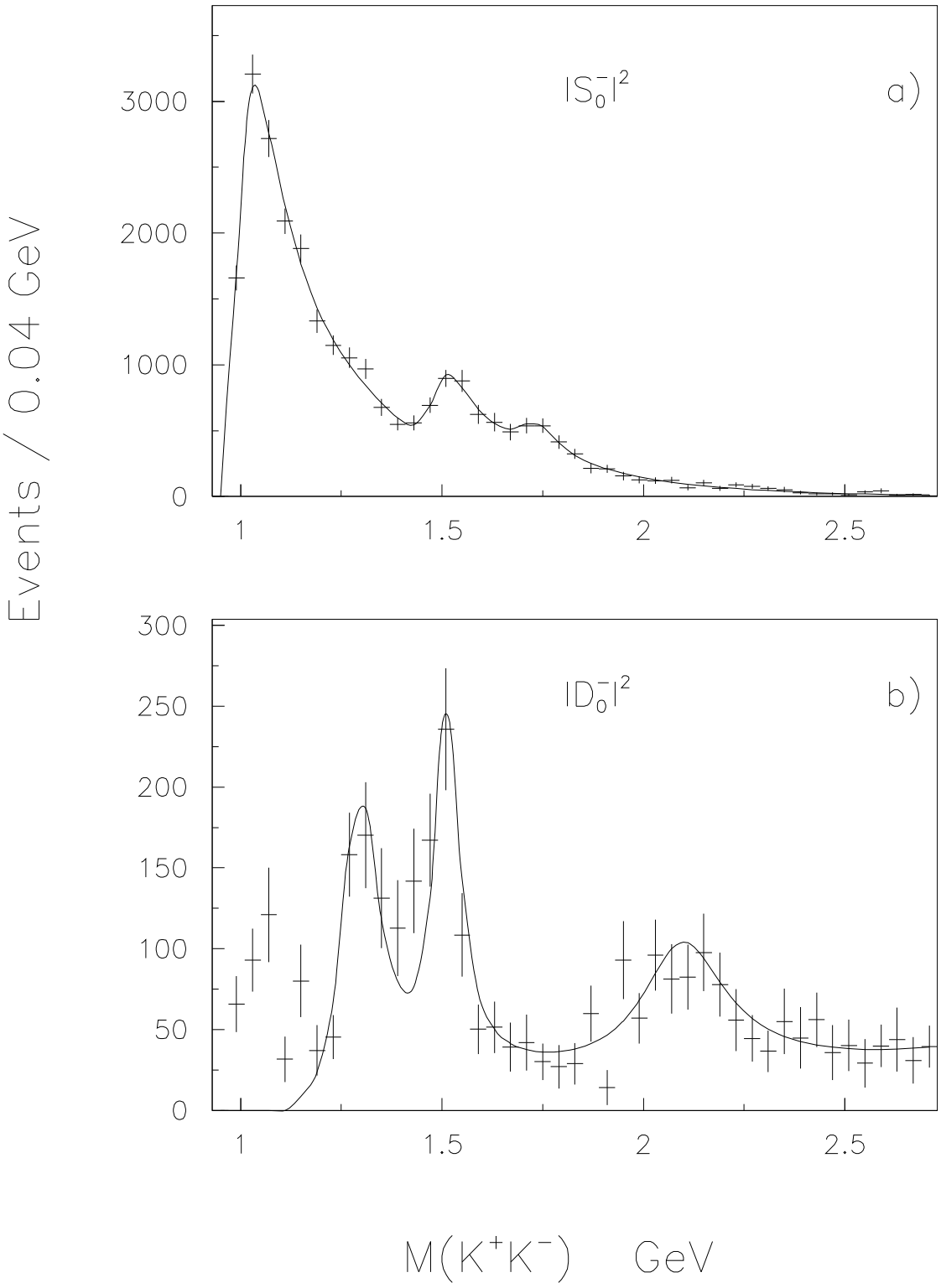
Events / 0.04 GeV
$|S_0^-|^2$
a)
3000
2000
1000
0
1
1.5
2
2.5
$|D_0^-|^2$
b)
300
250
200
150
100
50
0
1
1.5
2
2.5
$M(K^+K^-)$ GeV

Figure 4

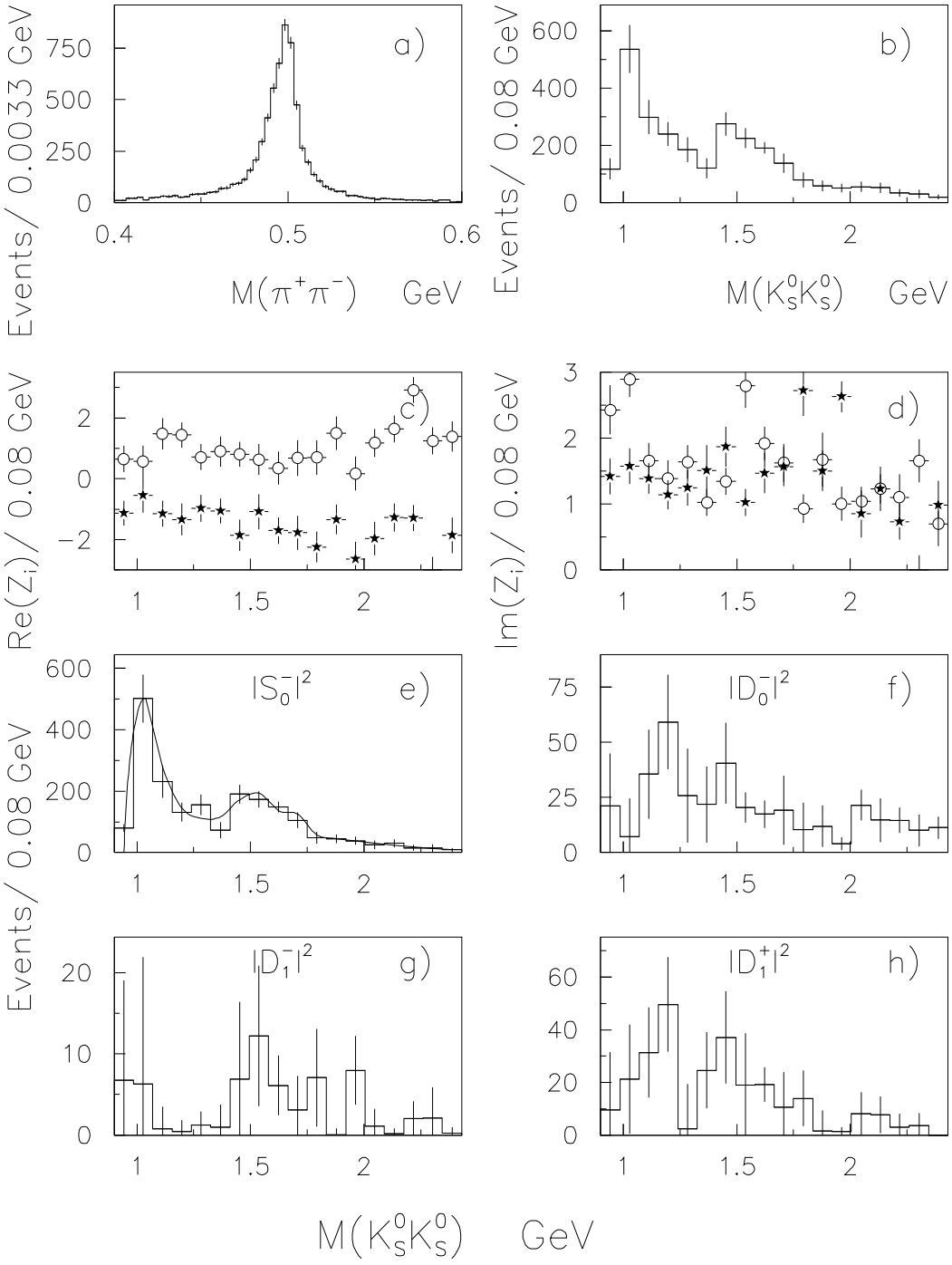
a)
b)
c)
d)
e)
f)
g)
h)
Events/ 0.0033 GeV
Events/ 0.08 GeV
Re(Z_i)/ 0.08 GeV
Im(Z_i)/ 0.08 GeV
M(π⁺π⁻) GeV
M(K⁰_sK⁰_s) GeV
|S⁻₀|²
|D⁻₀|²
|D⁻₁|²
|D⁺₁|²

Figure 5